

**Robust  $d_{x^2-y^2}$ -wave superconductivity of infinite-layer nickelates**Xianxin Wu,<sup>1,\*</sup>† Domenico Di Sante,<sup>1,\*</sup> Tilman Schwemmer<sup>1</sup>, Werner Hanke,<sup>1</sup> Harold Y. Hwang,<sup>2,3</sup> Srinivas Raghu,<sup>2,4,‡</sup> and Ronny Thomale<sup>1,§</sup><sup>1</sup>*Institut für Theoretische Physik und Astrophysik, Universität Würzburg, Am Hubland Campus Süd, 97074 Würzburg, Germany*<sup>2</sup>*Stanford Institute for Materials and Energy Sciences, SLAC National Accelerator Laboratory, Menlo Park, California 94025, USA*<sup>3</sup>*Department of Applied Physics, Stanford University, Stanford, California 94305, USA*<sup>4</sup>*Department of Physics, Stanford University, Stanford, California 94305, USA*

(Received 10 September 2019; revised manuscript received 3 February 2020; accepted 5 February 2020; published 24 February 2020)

Motivated by the recent observation of superconductivity in strontium-doped NdNiO<sub>2</sub>, we study the superconducting instabilities in this system from various vantage points. Starting with first-principles calculations, we construct two distinct tight-binding models, a simpler single-orbital as well as a three-orbital model, both of which capture the key low-energy degrees of freedom to varying degrees of accuracy. We study superconductivity in both models using the random phase approximation. We then analyze the problem at stronger coupling, and study the dominant pairing instability in the associated  $t$ - $J$  model limit. In all instances, the dominant pairing tendency is in the  $d_{x^2-y^2}$  channel, analogous to the cuprate superconductors.

DOI: [10.1103/PhysRevB.101.060504](https://doi.org/10.1103/PhysRevB.101.060504)

**Introduction.** The observation of superconductivity in the infinite-layer nickelate Nd<sub>1-x</sub>Sr<sub>x</sub>NiO<sub>2</sub> [1] resurrects some of the perennial questions in the field of unconventional superconductivity of the cuprates and related materials [2,3]. As nickel substitutes for copper in this system, the low-energy manifold consists primarily of the Ni-O plane. Therefore, we are invited to revisit whether copper itself is important for the superconductivity exhibited by the cuprates [4–9]. Furthermore, to date, magnetism has not been observed in the parent NdNiO<sub>2</sub> compound [10,11]. One may therefore question the extent to which close proximity to long-range antiferromagnetism is an essential ingredient in cuprate superconductivity.

To help address these questions, we have studied superconductivity from repulsive interactions in Nd<sub>1-x</sub>Sr<sub>x</sub>NiO<sub>2</sub>, adopting both weak- and strong-coupling approaches. Starting with a first-principles study of NdNiO<sub>2</sub>, and treating the effects of strontium doping as a rigid shift to the chemical potential, we have obtained tight-binding (TB) fits to the electronic structure. As Ni is isoelectronic to copper in this material, it has a  $d^9$  configuration and the low-energy physics is dominated by electrons in the Ni- $d_{x^2-y^2}$  orbital (see Fig. 1). There is, however, an additional strong hybridization with the  $5d$  orbitals of the rare-earth Nd element. As a consequence, there is a nonzero contribution to the low-energy physics from the Nd  $d_{z^2}$  and  $d_{xy}$  orbitals, which acts to introduce some distinction between this system and the infinite-layer cuprate material.

However, rather than speculating on the commonalities and differences of the infinite-layer cuprates and nickelates, we have instead chosen to study superconductivity in the nickelate material as a legitimate problem in its own right, one that is independent from the cuprates. The weak-coupling approach, while likely unreliable for normal-state properties, does tend to capture the primary property of interest, namely, the superconducting ground state itself and, in particular, the symmetry of the superconducting order parameter. We find robust  $d_{x^2-y^2}$ -wave superconductivity within the weak-coupling approach. We have obtained this pairing symmetry in two distinct tight-binding fits to the first-principles calculation, one which is a minimal one-orbital model consisting of the Ni  $d_{x^2-y^2}$  orbital, and a more realistic three-orbital model that includes the  $d_{z^2}$ ,  $d_{xy}$  orbitals of the Nd atom.

In reality, however, the system is likely located at intermediate coupling; it therefore becomes important to analyze the problem from complementary limits. With this in mind, we also analyze the  $t$ - $J$  model that results from the limit of strong Ni on-site interactions, and study superconductivity in this model within a mean-field approximation. Such methods led to the conclusion of  $d$ -wave pairing in the early days of cuprate physics [12], and we arrive at a similar conclusion in the present context. We also show that with the inclusion of the Nd electron pockets,  $d_{x^2-y^2}$  pairing stemming from the effective  $t$ - $J$  model is only weakly affected. While these electron pockets ultimately lead to metallic rather than Mott-insulating behavior in the parent compound, their impact on superconductivity appears to be rather weak. The fact that all limits studied here result in  $d_{x^2-y^2}$  pairing underlies the robustness of our conclusion.

This Rapid Communication is organized as follows. At first, we present the results of the first-principles computations, where we describe both the minimal single-band and

\*These authors equally contributed to the work.

†xianxinwu@gmail.com

‡sraghu@stanford.edu

§rthomale@physik.uni-wuerzburg.de

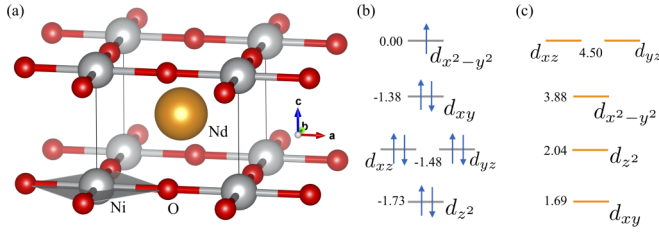


FIG. 1. (a) View of the crystal structure of NdNiO<sub>2</sub>. Ni, O, and Nd atoms are represented by gray, red, and orange spheres. The planar coordination in the NiO<sub>2</sub> is highlighted by a gray square. (b) The resulting crystal field is characterized by a top  $d_{x^2-y^2}$  orbital, which is singly occupied in a  $d^9$  electronic configuration. (c) Crystal field acting on the formally empty Nd  $d$  orbitals. In (b) and (c), the crystal-field levels are given in eV, with respect to the Ni  $d_{x^2-y^2}$ .

three-band tight-binding fits to the electronic structure. We then proceed to show our results for the pairing symmetry both in a random phase approximation (RPA) treatment of superconductivity from repulsive interactions, as well as from the analysis of a  $t$ - $J$  model description. Both complementary studies are carried out in three dimensions (3D), corresponding to the infinite-layer limit.

*First-principles analysis.* We performed first-principles calculations within the framework of the density functional theory (DFT) as implemented in the Vienna *ab initio* simulation package VASP [13–15]. The generalized gradient approximation, as parametrized by the Perdew-Burke-Ernzerhof generalized gradient approximation (PBE-GGA) functional for the exchange-correlation potential, was used by expanding the Kohn-Sham wave functions into plane waves up to an energy cutoff of 600 eV and sampling the Brillouin zone on a  $16 \times 16 \times 16$  regular mesh [16]. The growth of NdNiO<sub>2</sub> on a SrTiO<sub>3</sub> substrate is simulated by imposing an in-plane lattice constant  $a = 3.91$  Å and relative relaxed out-of-plane parameter  $c = 3.37$  Å [1]. The extraction of the three-orbital minimal model used to investigate the superconducting tendencies of NdNiO<sub>2</sub> was based on the Wannier functions formalism [17].

Figure 2 shows the single-particle band structure of NdNiO<sub>2</sub>, along with the orbital contributions relevant for the low-energy model description. Owing to a  $d^9$  electronic configuration in a peculiar +1 oxidation state for Ni, the crystal field imposed by the planar square coordination (Fig. 1) results in a high-lying nominally half-filled  $d_{x^2-y^2}$  orbital (red dots), featuring a predominantly two-dimensional character. Nonetheless, the delocalized and formally empty Nd  $5d$  states reside fairly low in energy, leading to a sizable hybridization with Ni  $3d$  bands, and to the appearance of electron pockets at the  $\Gamma$  and  $A = (\pi/a, \pi/a, \pi/c)$  [see Fig. 2(a)] points. Such pockets mainly display Nd  $d_{z^2}$  (yellow squares) and  $d_{xy}$  (blue diamonds) orbital contributions, respectively, and determine a concomitant self-doping of the large holelike Ni  $d_{x^2-y^2}$  Fermi surface.

Having established the contribution of the relevant orbitals to the low-energy physics of NdNiO<sub>2</sub>, we consider a three-orbital tight-binding (TB) model which includes long-range hopping terms. We introduce the operator  $\psi_{\mathbf{k}\sigma}^\dagger = [c_{1\sigma}^\dagger(\mathbf{k}), c_{2\sigma}^\dagger(\mathbf{k}), c_{3\sigma}^\dagger(\mathbf{k})]$ , where  $c_{\alpha\sigma}^\dagger(\mathbf{k})$  is a fermionic creation operator with  $\sigma$  and  $\alpha$  denoting spin and orbital indices,

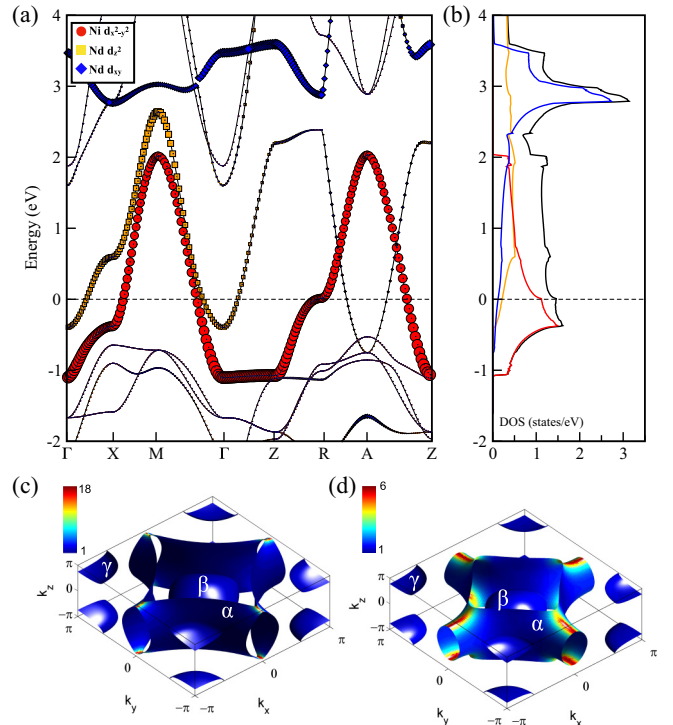


FIG. 2. (a) First-principles band structure and (b) density of states of NdNiO<sub>2</sub> with lattice parameters forced by the commensuration to the SrTiO<sub>3</sub> substrate. The red (Ni  $d_{x^2-y^2}$ ), yellow (Nd  $d_{z^2}$ ), and blue (Nd  $d_{xy}$ ) symbols emphasize the relevant orbitals that contribute to the low-energy description. In (b) the black curve refers to the sum of the individual contributions. Views of the Fermi surface of NdNiO<sub>2</sub> at (c) pristine filling ( $n = 1.0$ ) and (d) upon 0.2 hole doping ( $n = 0.8$ ). The color scale reports the momentum dependence of the inverse Fermi velocity  $[1/v_F(\mathbf{k})]$ , which is a measure of the DOS. The  $\alpha$  Fermi surface displays a van Hove feature evolving from the  $k_z = 0$  cut to the  $k_z = \pi$  cut, where it changes from a hole pocket around the  $M$  point in the  $k_z = 0$  plane to an electron pocket around the  $Z$  point in the  $k_z = \pi$  plane.

respectively. The orbital index  $\alpha = 1, 2, 3$  represents the Nd  $d_{z^2}$  for 1, the Nd  $d_{xy}$  for 2, and the Ni  $d_{x^2-y^2}$  for 3. The tight-binding Hamiltonian can be written as

$$H_{\text{TB}} = \sum_{\mathbf{k}\sigma} \psi_{\mathbf{k}\sigma}^\dagger h(\mathbf{k}) \psi_{\mathbf{k}\sigma}, \quad (1)$$

where  $h(\mathbf{k})$  is given in Ref. [18], along with the corresponding parameters extracted from a downfolding of the first-principles band structure onto a set of localized Wannier functions. With the above parameters, the obtained band structure fits are given in Ref. [18] and reach a good agreement between DFT and the effective TB bands. Near the Fermi level, the density of states (DOS) is dominantly attributed to the Ni  $d_{x^2-y^2}$  orbital, as shown in Fig. 2(b). Further considering the relatively weak interaction effects in the  $5d$  orbitals of Nd, the dominant correlation effects must derive from the  $3d$   $d_{x^2-y^2}$  orbital of Ni in NdNiO<sub>2</sub>. These conclusions are consistent with previous [7,8] as well as concurrent [19] first-principles calculations of this system.

The resulting three-dimensional (3D) Fermi surfaces are shown in Figs. 2(c) and 2(d) for the fillings  $n = 1.0$  and

$n = 0.8$ . For the former case, there is an almost cylindrical, nondispersive in  $k_z$ , holelike pocket  $\alpha$ , and two small electron-like pockets  $\beta$  and  $\gamma$  around the  $\Gamma$  and A points, respectively. With 0.2 hole doping, the electron Fermi surfaces shrink. For the hole pocket, van Hove singularities are reached near the  $k_z = \pi$  plane, and its density of states increases considerably along with enhanced nesting, as shown by the red curve in Fig. 2(b). The three-dimensional character of the obtained Fermiology is an essential distinguishing aspect from the infinite-layer cuprates. Within a weak-coupling framework of superconductivity, such an enhancement of the density of states available for pairing as obtained for hole doping in the nickelates typically results in a concomitant increase of the superconducting temperature. The largest contribution to the density of states arises from the large non- $k_z$ -dispersive Ni  $d_{x^2-y^2}$  pocket, suggesting that, to some approximation, it likely plays a significant role in the superconducting transition.

*Weak-coupling analysis.* In order to investigate the pairing symmetry of NdNiO<sub>2</sub>, we first consider a weak-coupling limit of the problem. Weak coupling can either be interpreted as the strictly analytically controlled perturbative limit of interactions [20–22] or, in a less restrictive meaning, as the itinerant electronic limit in which a diagrammatic, e.g., RPA, treatment of interactions is adopted starting from the bare or effective electronic band structure. Such or related approaches, while less controlled than the strictly perturbative weak-coupling limit, are more physically motivated, and result in qualitatively similar conclusions for pairing strengths in the system. They have enjoyed significant phenomenological success in describing unconventional superconductivity [23]. For instance, in both the weak-coupling and RPA treatments of the single-band Hubbard model, the dominant pairing tendency near half filling is in the  $d_{x^2-y^2}$  channel [24,25]. A perturbative combined diagrammatic inclusion of particle-particle and particle-hole contributions could be reached by the employment of functional renormalization group [26,27] in order to further sophisticate the RPA treatment. For the case at hand, however, the absence of magnetic order combined with the enhanced feasibility in treating three-dimensional band structures renders the RPA approach most preferable at this stage of our weak-coupling analysis.

In our RPA calculations, we consider on-site Hubbard intra- and interorbital repulsion, Hund's coupling, as well as pair-hopping interactions,

$$\begin{aligned}
 H_{\text{int}} = & U_{\text{Ni}} \sum_i n_{i3\uparrow} n_{i3\downarrow} + U_{\text{Nd}} \sum_{i\mu} n_{i\mu\uparrow} n_{i\mu\downarrow} \\
 & + U'_{\text{Nd}} \sum_{i,\mu<\nu} n_{i\mu} n_{i\nu} + J_{\text{Nd}} \sum_{i,\mu<\nu,\sigma\sigma'} c_{i\mu\sigma}^\dagger c_{i\nu\sigma'}^\dagger c_{i\mu\sigma'} c_{i\nu\sigma} \\
 & + J'_{\text{Nd}} \sum_{i,\mu\neq\nu} c_{i\mu\uparrow}^\dagger c_{i\mu\downarrow}^\dagger c_{i\nu\downarrow} c_{i\nu\uparrow}, \quad (2)
 \end{aligned}$$

where  $n_{i\alpha} = n_{\alpha\uparrow} + n_{\alpha\downarrow}$ ,  $\mu, \nu = 1, 2$ ,  $U_{\text{Ni}}$  is the Coulomb repulsion for the Ni site, thus acting on the third orbital in the notation of Eq. (1).  $U_{\text{Nd}}$ ,  $U'_{\text{Nd}}$ ,  $J_{\text{Nd}}$ , and  $J'_{\text{Nd}}$  represent the on-site intra- and interorbital repulsion and the on-site Hund's coupling and pair-hopping terms for the Nd site, respectively. For simplicity, we have chosen the same value of  $U$  for

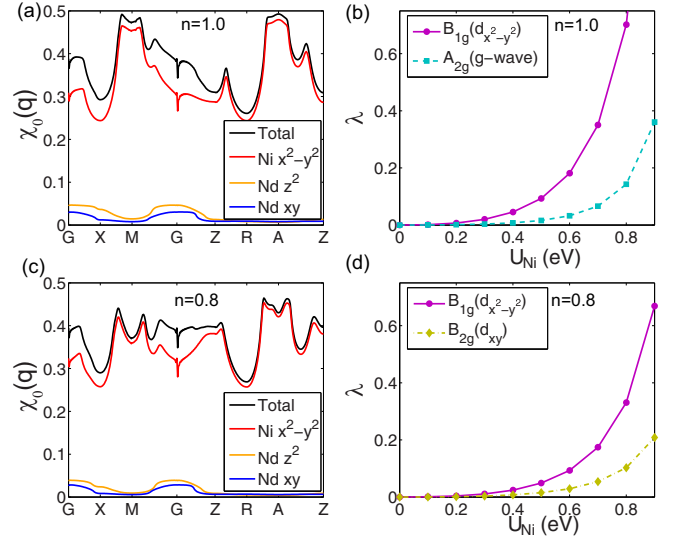


FIG. 3. Bare susceptibility (left panels) and pairing eigenvalues as a function of the interaction  $U_{\text{Ni}}$  (right panels) for electron filling  $n = 1.0$  (top row) and  $n = 0.8$  (bottom row), respectively. Here, we adopt  $U_{\text{Ni}} = U_{\text{Nd}}$  and  $J_{\text{Nd}}/U_{\text{Nd}} = 0.15$ .

both the Nd and Ni  $d$  orbitals. This initial choice does not fundamentally affect the effective BCS coupling that arises at order  $U^2$ , as it is weighted by the susceptibility of each orbital. As such, the BCS couplings at low energies systematically are significantly different for Nd and Ni electrons. We use the Kanamori relations  $U_{\text{Nd}} = U'_{\text{Nd}} + 2J_{\text{Nd}}$  and  $J_{\text{Nd}} = J'_{\text{Nd}}$ .

Figure 3 displays the bare susceptibilities for  $n = 1.0$  and  $n = 0.8$  filling, respectively. In both cases, similar to cuprates, the dominant peaks are located around the  $M$  and  $A$  points, indicating intrinsic antiferromagnetic fluctuations. These peaks get significantly enhanced upon including interactions at the RPA level. The prominent features in the orbital-resolved susceptibility are that the peaks around  $M$  and  $A$  are dominantly attributed to the Ni  $d_{x^2-y^2}$  orbital while the contribution of Nd  $d_{xy}$  and  $d_{z^2}$  reaches its maximum around  $\Gamma$ . Based on the analysis of the susceptibility, the  $d_{x^2-y^2}$  band will play the dominant role in promoting correlation phenomena, including superconductivity and, if commensurate filling of this band were reached, possible magnetic ordering.

As a systematic methodological feature, when the interaction is greater than a critical value  $U_c$  (1.1 eV in our case), the spin susceptibility within RPA diverges and indicates a spin-density-wave (SDW) instability. Note that as a matter of principle,  $U_c$  should be interpreted as a phenomenological parameter that does not allow an immediate quantitative connection with the bare unrenormalized interaction strength. Below  $U_c$ , superconductivity emerges triggered by spin fluctuations. We perform RPA calculations to study the possible pairing symmetries within a  $40 \times 40 \times 20$   $k$  mesh, energy window  $\Delta E = 0.02$  eV around the Fermi level, and inverse temperature  $\beta = 50$  eV<sup>-1</sup>, and have checked the convergence of pairing strength with respect to the  $k$  mesh and  $\Delta E$ . With the above parameters, the numbers of the representative momentum points on the Fermi surface are 1038 and 1088 for  $n = 1.0$  and  $n = 0.8$ , respectively. From the susceptibility,

we can expect the dominant pairing state to be  $d_{x^2-y^2}$  wave (more details on the RPA are provided in the Supplemental Material [18]). As the effective low-energy interaction parameters remain as of yet largely undetermined for infinite-layer nickelates, we have performed our RPA calculations within a large region of parameter space, and consistently found the dominant pairing to be unchanged, and, in particular, largely insensitive to the bare initial value  $U_{\text{Nd}}$ . The obtained pairing eigenvalues as a function of interaction strength  $U$  for  $n = 1.0$  and  $n = 0.8$  are displayed in Fig. 3. We find that the  $d_{x^2-y^2}$  pairing state is dominant, and that the gap functions are considerably smaller on the two small spherical Fermi surfaces. This is consistent with the fact that both the dominant density of states and pairing interactions reside on the Ni  $d_{x^2-y^2}$  orbital.

*Pairing in the  $t$ - $J$  model.* Similar to cuprates, the nickelates represent an intermediately coupled system, and it becomes important to “triangulate” the pairing problem from various limits to see if our conclusions are indeed robust. From a strong-coupling perspective, the cuprates have been addressed within an effective  $t$ - $J$  model which is either obtained from the Gutzwiller projection of a single-band Hubbard model or the low-energy perturbative description of the three-band Hubbard model involving the Cu  $d_{x^2-y^2}$  and the planar O  $p_{x,y}$  orbitals [28]. As of yet, it is unclear whether the charge transfer gap in the nickelates [19] allows for a Zhang-Rice-type Ni-O singlet complex of two holes as a suitable effective description. Still, approaching the nickelates from a related angle, we adopt the  $t$ - $J$  model reduced to the Ni  $d_{x^2-y^2}$  orbital. In doing so, we describe a strong-coupling limit of the doped Ni  $d_{x^2-y^2}$  band by constraining ourselves to the in-plane and out-of-plane antiferromagnetic couplings between the Ni spins,

$$H_J = \sum_{\langle ij \rangle} J_{ij} \left( \mathbf{S}_{i3} \mathbf{S}_{j3} - \frac{1}{4} n_{i3} n_{j3} \right), \quad (3)$$

where  $\mathbf{S}_{i3} = \frac{1}{2} c_{i3\sigma}^\dagger \boldsymbol{\sigma}_{\sigma\sigma'} c_{i3\sigma'}$  is the local spin operator and  $n_{i3}$  is the local density operator for the Ni  $d_{x^2-y^2}$  orbital.  $\langle ij \rangle$  denotes the in-plane and out-of-plane nearest neighbor (NN). The in-plane coupling is  $J_x = J_y = J_1$  and the out-of-plane coupling is  $J_2$ . We investigate the pairing state for an extended range of doping levels. We simplify the analysis by relaxing the double-occupancy constraint on this  $t$ - $J$  model, perform a mean-field decoupling, and solve the self-consistent gap equations [18]. We find that  $d_{x^2-y^2}$  pairing is always the dominant order within extended parameter ranges of  $J_1$  and  $J_2$ , and that  $J_2$  has a negligible effect on the gap. Figure 4(a) shows the representative superconducting gap of the  $d_{x^2-y^2}$  pairing as a function of doping with  $J_1 = J_2 = 0.1$  eV. We find that there is a superconducting dome and the gap reaches the maximum upon 0.1 hole doping. Electron doping, by reducing the contribution of the Ni  $d_{x^2-y^2}$  orbital, will significantly suppress superconductivity. Instead, beyond optimal doping, further hole doping will only slightly suppress the superconducting gap, implying to expect an extended  $T_c$  dome feature on the hole-doped side. The 3D gap function of the obtained  $d_{x^2-y^2}$ -wave pairing is displayed in Fig. 4(b) at 0.2

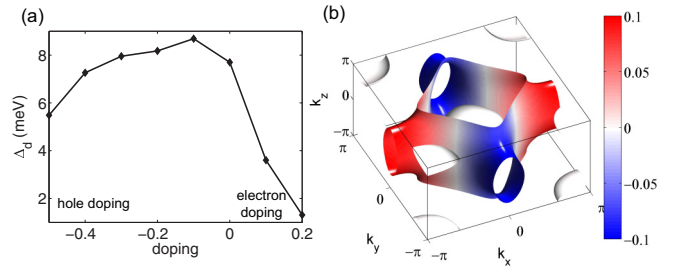


FIG. 4. (a) The  $d_{x^2-y^2}$ -wave gap as a function doping with  $J_1 = J_2 = 0.1$  eV. Positive (negative) values relate to electron (hole) doping. (b) Superconducting gap for  $d_{x^2-y^2}$ -wave pairing. In the calculations, a  $k$  mesh of  $100 \times 100 \times 50$  has been adopted.

hole doping, where the gaps on the spherical Fermi surfaces from Nd atoms almost vanish. Our findings from a  $t$ - $J$  model analysis thus are consistent with our weak-coupling analysis.

*Discussion.* We have studied the infinite-layer nickelate NdNiO<sub>2</sub> and have found that the dominant pairing instability is in the  $d_{x^2-y^2}$  channel, which places this system in close analogy with cuprate superconductors. As a consequence of the pairing symmetry, we expect nodes on the Fermi surface, the evidence for which can be found in low-temperature heat capacity [29], penetration depth [30] measurements, quasi-particle interference studies [31], and more directly, from phase-sensitive studies [32,33].

In the future, it will be interesting to study the role of the Nd itinerant electrons in conjunction with the local moments of the Ni sites. It is thus tempting to invoke the analogy with heavy fermion systems, and to view the physics of the infinite-layer nickelate from the vantage point of the Kondo lattice. In this context, it is reasonable to presume that the effect of strontium doping involves more complex phenomena than a simple rigid shift of the Fermi level. Furthermore, even though an electronically mediated pairing mechanism may appear likely judging from the current experimental evidence, the impact of electron-phonon coupling will be vital to gaining a deeper understanding of the material [34]. We wish to pursue such questions in future studies.

*Note added.* Recently, we became aware of an independent study of electronic structure and pairing instabilities in infinite-layer nickelates [35]. This study makes use of a variant of the RPA method [fluctuational exchange (FLEX) approximation] and finds similar conclusions for pairing.

*Acknowledgments.* The work in Würzburg is funded by the Deutsche Forschungsgemeinschaft (DFG, German Research Foundation) through Project-ID 258499086 - SFB 1170 and through the Würzburg-Dresden Cluster of Excellence on Complexity and Topology in Quantum Matter – *ct.qmat* Project-ID 39085490 - EXC 2147. H.Y.H. and S.R. are supported by the DOE Office of Basic Energy Sciences, Contract No. DEAC02-76SF00515. We gratefully acknowledge the Gauss Centre for Supercomputing e.V. [36] for funding this project by providing computing time on the GCS Supercomputer SuperMUC at Leibniz Supercomputing Centre [37].

- [1] D. Li, K. Lee, B. Y. Wang, M. Osada, S. Crossley, H. R. Lee, Y. Cui, Y. Hikita, and H. Y. Hwang, *Nature (London)* **572**, 624 (2019).
- [2] P. A. Lee, N. Nagaosa, and X.-G. Wen, *Rev. Mod. Phys.* **78**, 17 (2006).
- [3] B. Keimer, S. A. Kivelson, M. R. Norman, S. Uchida, and J. Zaanen, *Nature (London)* **518**, 179 (2015).
- [4] Y. Maeno, H. Hashimoto, K. Yoshida, S. Nishizaki, T. Fujita, J. Bednorz, and F. Lichtenberg, *Nature (London)* **372**, 532 (1994).
- [5] J. Chaloupka and G. Khaliullin, *Phys. Rev. Lett.* **100**, 016404 (2008).
- [6] Y. K. Kim, N. Sung, J. Denlinger, and B. Kim, *Nat. Phys.* **12**, 37 (2016).
- [7] V. I. Anisimov, D. Bukhvalov, and T. M. Rice, *Phys. Rev. B* **59**, 7901 (1999).
- [8] K.-W. Lee and W. E. Pickett, *Phys. Rev. B* **70**, 165109 (2004).
- [9] P. Hansmann, X. Yang, A. Toschi, G. Khaliullin, O. K. Andersen, and K. Held, *Phys. Rev. Lett.* **103**, 016401 (2009).
- [10] M. Hayward, M. Green, M. Rosseinsky, and J. Sloan, *J. Am. Chem. Soc.* **121**, 8843 (1999).
- [11] M. Hayward and M. Rosseinsky, *Solid State Sci.* **5**, 839 (2003).
- [12] G. Kotliar and J. Liu, *Phys. Rev. B* **38**, 5142 (1988).
- [13] G. Kresse and J. Furthmüller, *Phys. Rev. B* **54**, 11169 (1996).
- [14] G. Kresse and D. Joubert, *Phys. Rev. B* **59**, 1758 (1999).
- [15] P. E. Blöchl, *Phys. Rev. B* **50**, 17953 (1994).
- [16] J. P. Perdew, K. Burke, and M. Ernzerhof, *Phys. Rev. Lett.* **77**, 3865 (1996).
- [17] A. A. Mostofi, J. R. Yates, Y.-S. Lee, I. Souza, D. Vanderbilt, and N. Marzari, *Comput. Phys. Commun.* **178**, 685 (2008).
- [18] See Supplemental Material at <http://link.aps.org/supplemental/10.1103/PhysRevB.101.060504> for the details about the tight binding model, random phase approximation and t-J model calculations.
- [19] A. S. Botana and M. R. Norman, *Phys. Rev. X* **10**, 011024 (2020).
- [20] W. Kohn and J. Luttinger, *Phys. Rev. Lett.* **15**, 524 (1965).
- [21] S. Raghu, S. A. Kivelson, and D. J. Scalapino, *Phys. Rev. B* **81**, 224505 (2010).
- [22] W. Cho, R. Thomale, S. Raghu, and S. A. Kivelson, *Phys. Rev. B* **88**, 064505 (2013).
- [23] D. J. Scalapino, *Rev. Mod. Phys.* **84**, 1383 (2012).
- [24] D. J. Scalapino, E. Loh, and J. E. Hirsch, *Phys. Rev. B* **34**, 8190 (1986).
- [25] K. Miyake, S. Schmitt-Rink, and C. M. Varma, *Phys. Rev. B* **34**, 6554 (1986).
- [26] W. Metzner, M. Salmhofer, C. Honerkamp, V. Meden, and K. Schönhammer, *Rev. Mod. Phys.* **84**, 299 (2012).
- [27] C. Platt, W. Hanke, and R. Thomale, *Adv. Phys.* **62**, 453 (2013).
- [28] F. C. Zhang and T. M. Rice, *Phys. Rev. B* **37**, 3759 (1988).
- [29] K. A. Moler, A. Kapitulnik, D. J. Baar, R. Liang, and W. N. Hardy, *J. Phys. Chem. Solids* **56**, 1899 (1995).
- [30] W. N. Hardy, D. A. Bonn, D. C. Morgan, R. Liang, and K. Zhang, *Phys. Rev. Lett.* **70**, 3999 (1993).
- [31] J. E. Hoffman, K. McElroy, D.-H. Lee, K. M. Lang, H. Eisaki, S. Uchida, and J. C. Davis, *Science* **297**, 1148 (2002).
- [32] D. J. Van Harlingen, *Rev. Mod. Phys.* **67**, 515 (1995).
- [33] C. C. Tsuei and J. R. Kirtley, *Rev. Mod. Phys.* **72**, 969 (2000).
- [34] Y. Nomura, M. Hirayama, T. Tadano, Y. Yoshimoto, K. Nakamura, and R. Arita, *Phys. Rev. B* **100**, 205138 (2019).
- [35] H. Sakakibara, H. Usui, K. Suzuki, T. Kotani, H. Aoki, and K. Kuroki, *arXiv:1909.00060*.
- [36] [www.gauss-centre.eu](http://www.gauss-centre.eu)
- [37] [www.lrz.de](http://www.lrz.de)